Kinetic Studies in Aqueous Solutions of Cobalt(II)–Ethylenediamine, –Malonate, and –Glycinate Complexes

Károly Micskei * and **István Nagypál**
Institute of Inorganic and Analytical Chemistry, Lajos Kossuth University, H-4010 Debrecen, Hungary

The dynamics of equilibria in aqueous solutions of cobalt(II)–ethylenediamine (en), –malonate (mal), and –glycinate (glyO) systems have been investigated by measuring the paramagnetic relaxation rate and shift of the CH_2 ligand protons over a wide range of complex formation. The formation rate constants ($dm^3\ mol^{-1}\ s^{-1}$) of the cobalt parent complexes at 25 °C and $I = 1$ mol dm^{-3} KCl are: $k_2^{en} = 3.0 \times 10^7$, $k_3^{en} = 1.1 \times 10^7$, $k_1^{mal} = 6.9 \times 10^7$, $k_2^{mal} = 1.6 \times 10^7$, $k_2^{glyO} = 2.2 \times 10^6$, and $k_3^{glyO} = 6.4 \times 10^5$. Kinetic evidence is given for the formation of $[Co(Hen)]^{3+}$, $[Co(Hmal)]^+$, and $[Co(mal)_3]^{4-}$ complexes. The 'carboxyl-displacement' mechanism was used to interpret the interaction between $[Co(glyO)_3]^-$ and the free $glyO^-$ ligand. The complex-formation kinetics of some complexes of Co^{2+} and Fe^{2+} were compared and the similarities and differences are discussed.

The dynamics of equilibria in aqueous solutions of some chromium(II) and iron(II) complexes have been described in our earlier papers,[1–3] using the n.m.r. relaxation method. The extension of the use of paramagnetic n.m.r. relaxation to these complexes required the generalization of the Swift–Connick equations[4] for multisite systems, taking into account the '$\Delta\omega$' relaxation mechanism, too.[2]

The equilibrium properties of some iron(II) complexes have also been measured.[5] The stability constants of the complexes of Fe^{2+} and Co^{2+} were compared and the similarities and differences discussed. The fundamental co-ordination properties of Fe^{2+} and Co^{2+} were found to be similar but the analysis of the equilibrium data indicated a greater degree of covalent bonding in the cobalt complexes as a consequence of the different electron structures.

The kinetic properties of the cobalt(II)–glycinate (glyO) and –malonate (mal) systems were studied in detail earlier. Using the chemical relaxation method (*T*-jump) the formation rate constants of the complexes $[Co(glyO)]^+$, $[Co(glyO)_2]$, $[Co(glyO)_3]^-$, and [Co(mal)] were measured.[6–9] The kinetic properties of the remaining water molecules in the co-ordination sphere of some glycinate and malonate complexes were investigated using the ^{17}O n.m.r. relaxation method.[9,10] Only n.m.r. relaxation kinetic data are available for the cobalt(II)–ethylenediamine (en) system where the formation rate constant of the complex $[Co(en)_3]^{2+}$ was determined.[11,12]

To be able to compare the kinetic results obtained by the n.m.r. and chemical relaxation techniques, we have studied the cobalt(II)–glycinate system because the chemical relaxation results seem to be correct, whereas published data are rather incomplete for the cobalt(II)–malonate and –ethylenediamine systems. Nevertheless, the complementary application of chemical and n.m.r. relaxation methods is providing new results for the earlier studied systems, too.

Taking into account our earlier results for the iron(II)–ethylenediamine, –malonate, and –glycinate complexes[2] based on the same n.m.r. relaxation method, in this paper the formation kinetics of complexes of Co^{2+} and Fe^{2+} will be compared and the similarities and differences discussed.

Experimental

Equilibrium Studies.—The equilibria in solutions of cobalt(II)–ethylenediamine, –malonate, and –glycinate systems are well known;[13] we have repeated these studies only to get data under the conditions used in the relaxation studies. A Radiometer PH M-52 pH-meter equipped with a GK 2301 B combined electrode, calibrated for $-\log[H^+]$ according to Irving *et al.*,[14] was used for pH-metric and a Beckman Acta M4 photometer for spectrophotometric measurements. The measurements were carried out at 25 ± 0.1 °C using $I = 1.0$ mol dm^{-3}, adjusted with KCl. The samples (25.00 cm^3) were titrated with KOH solution under argon gas. Before the measurements the change in the ionic strength during the titrations was calculated and on this basis the appropriate quantity of KCl was added to the sample and when necessary to the KOH solution. The formation constants calculated using the program PSEQUAD[15] are collected in Table 1.

Table 1. Protonation constants of the ligands and formation constants (log β_i) of the cobalt(II) complexes (25 °C, $I = 1$ mol dm^{-3} KCl)

	L		
Complex	glyO	en	mal
HL	9.69	10.14	5.09
H_2L	12.15	17.53	7.71
[Co(HL)]	9.31 ± 0.02 *		6.39 ± 0.04
[CoL]	4.51 ± 0.01	5.68 ± 0.01	2.73 ± 0.02
$[CoL_2]$	8.26 ± 0.01	10.39 ± 0.01	4.57 ± 0.03
$[CoL_3]$	10.59 ± 0.01	13.95 ± 0.01	

* Determined spectrophotometrically.

The cobalt(II)–glycinate system was studied at a relatively high ligand excess ($c_{glyO} = 1.5000$, $0.004 < c_{Co} < 0.05$ mol dm^{-3}), because the complex formation occurs in the pH range where protonation of the ligand does not have a significant buffer effect.[16] This is not the case in the corresponding malonate and ethylenediamine systems; thus commensurable ligand-to-metal concentration ratios had to be used to get reliable equilibrium data in these systems ($0.04 < c_{en} < 0.2$, $0.008 < c_{Co} < 0.05$; $0.02 < c_{mal} < 0.1$, $0.008 < c_{Co} < 0.05$ mol dm^{-3}).

It has already been demonstrated[17] that the measured relaxation data may be profoundly influenced by kinetically rather active minor species, which may avoid detection in the

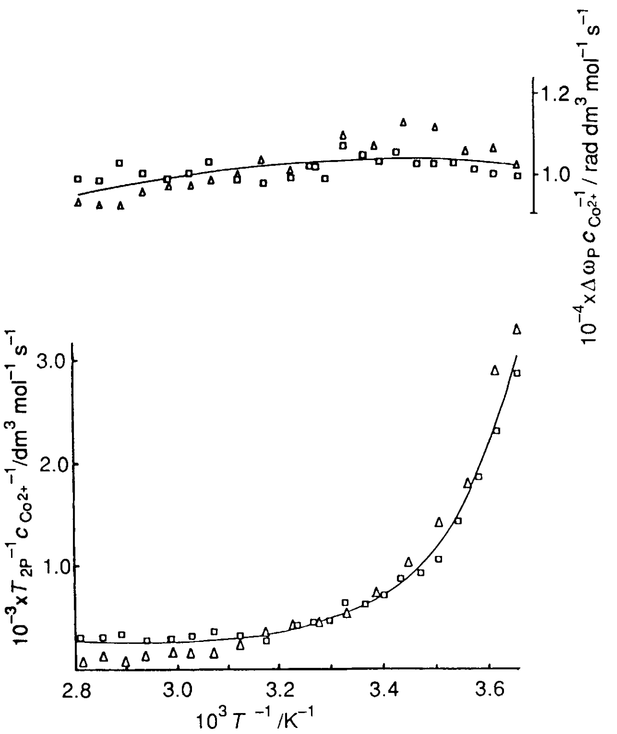

Figure 1. Temperature dependence of the paramagnetic relaxation rate and shift in an aqueous solution of Co^{2+} normalized for the total metal concentrations, together with the calculated curves; $P_{Co^{2+}} = 5.912 \times 10^{-3}$ (△) and 8.867×10^{-3} (□)

usual equilibrium analysis. The formation of the protonated complex in the cobalt(II)–malonate system was easily found from the pH-metric data. The complex $[Co(gly)]^{2+}$ was detected photometrically at pH 3.25, $c_{Co^{2+}} = 4.29 \times 10^{-2}$ mol dm^{-3} in the total concentration range $0.05 < c_{glyO} < 2.0$ mol dm^{-3} where only the Co^{2+} ion and the $[Co(gly)]^{2+}$ complex are dominant. The net absorbance is given by the linear combination of those of the two coloured species: $A = \varepsilon_{Co}[Co^{2+}] + \varepsilon_{Co(gly)}[Co(gly)^{2+}]$.

Using the program PSEQUAD the formation constants of the $[Co(gly)]^{2+}$ complex were determined (see Table 1). The formation constants for the parent complexes agree well with data published earlier,[13] but no data for the $[Co(gly)]^{2+}$ complex have yet been reported.

Further spectrophotometric equilibrium studies were carried out at high ligand excess, where pH-metry cannot be applied. No $[Co(mal)_3]^{4-}$ complex was detected up to $[mal^{2-}] = 0.5$ mol dm^{-3} and only CoL_3 type complexes were detected up to [en] or $[glyO^-] \approx 1.0$ in the ethylenediamine- and glycine-containing systems.

N.M.R. Studies.—All the n.m.r. spectra were recorded on a Bruker WP 200 SY spectrometer (operating at 200 MHz for protons). The chemical shifts were referenced to 3-(trimethylsilyl)propanesulphonic acid sodium salt). Experimental T_2 values were calculated from the half-widths of the n.m.r. signals.

For the n.m.r. relaxation measurements a special titration method was applied. The samples (5.00 cm^3) were prepared in the n.m.r. tube (diameters 1.00 and 20 cm) and deoxygenated with argon gas. The tube was closed with a special n.m.r. pressure cap ensuring a small overpressure of inert gas. The KOH solution was injected by an automatic burette fitted with a syringe piercing the pressure cap.

The measurements were carried out at 25 ± 1 °C unless otherwise stated. The ionic strength during the titrations was adjusted to $I = 1.0$ mol dm^{-3}. Before the titrations the ionic strength of the samples was calculated (because of the high concentration of the charged species in the samples and the considerable dilution) and the appropriate quantity of KCl was added to the sample and to the KOH solution.

The measured linewidths and shifts were corrected for the diamagnetism (measured in the absence of Co^{2+}) of the protons according to equations (1) and (2), where T_{2P}^{-1}, $\Delta\omega_P$ are the

$$T_{2P}^{-1} = \Pi(\Delta\nu_{\frac{1}{2}m} - \Delta\nu_{\frac{1}{2}d})\ \mathrm{s}^{-1} \qquad (1)$$

$$\Delta\omega_P = 2\Pi(\Delta\omega_m - \Delta\omega_d)\ \mathrm{rad\ s}^{-1} \qquad (2)$$

paramagnetic contribution to the relaxation rate and the shift, $\Delta\nu_{\frac{1}{2}m}$, $\Delta\omega_m$ are the measured linewidth at half-height and the measured resonance frequency in a solution of the cobalt complex, and $\Delta\nu_{\frac{1}{2}d}$, $\Delta\omega_d$ are the measured linewidth and the measured resonance frequency in the absence of Co^{2+} ion.

The experimental data measured in the absence of Co^{2+} (the temperature and pH dependence of the resonances of the H_2O and CH_2 protons) were used for the evaluation of the metal complex systems.

The concentration distributions of the species were calculated using the program PSEQUAD. For calculation of the kinetic parameters a computer program was used based on the generalized Swift–Connick equations[2] which can evaluate relaxation data measured for solutions containing several paramagnetic species.

Results and Discussion

Relaxation Mechanism of the Nucleus in the Co-ordination Sphere of Co^{2+}.—The correct interpretation of the relaxation data required knowledge of the relaxation mechanism of the water and the CH_2 protons of the ligands in the co-ordination sphere of the Co^{2+} ion.

Paramagnetic relaxation of the water protons. The water exchange rate between $[Co(H_2O)_6]^{2+}$ and bulk water has already been investigated by a number of authors using ^{17}O n.m.r. spectroscopy.[4,10,18]

The relaxation mechanism of the water protons in the co-ordination sphere of Co^{2+} was studied as suggested by Swift and Connick.[4] The temperature dependence of the paramagnetic relaxation rate and shift of the H_2O protons were measured in an aqueous solution of Co^{2+} (see Figure 1). For the simultaneous evaluation of the relaxation rate and shift data the temperature dependences of the Swift–Connick equations were used [$\tau_M = (h/kT)\exp(\Delta H^\ddagger/TR - \Delta S^\ddagger/R)$, $\Delta\omega_M/\omega_O = \alpha/T$, $T_{2M} = B \cdot \exp(C/RT)$; see ref. 4] and the best fit was reached when the relation $T_{2M}^{-1} \ll \Delta\omega_M$ was applied [equations (3) and (4)], where P_M is a molar ratio of the co-ordinated nucleus, *e.g.*

$$T_{2P}^{-1} = \frac{P_M \tau_M^{-1} \Delta\omega_M^2}{(\tau_M^{-2} + \Delta\omega_M^2)} = P_M r_{T2}^{-1} \qquad (3)$$

$$\Delta\omega_P = \frac{P_M \tau_M^{-2} \Delta\omega_M}{(\tau_M^{-2} + \Delta\omega_M^2)} = P_M r_\omega \qquad (4)$$

$P_{CoL_i} = i[CoL_i]/c_L$ (i is the co-ordination number of the ligand and c_L is the total ligand concentration), r_{T2}^{-1} and r_ω are the appropriate relaxation contributions of the paramagnetic species. The effect of the outer sphere (r_{os}) was taken into account with the only concentration-dependent parameter [equation (5)].

$$T_{2P}^{-1} = P_M[r_{T2}^{-1}(T) + r_{os}] \qquad (5)$$

The results of the calculation together with the earlier determined parameters for Fe^{2+} are collected in Table 2. The conclusion is that the paramagnetic relaxation in aqueous solutions of Co^{2+} and Fe^{2+} detected for the water protons can be attributed to the change in the resonance frequency ('$\Delta\omega$' mechanism). The proton and water exchange rates determined for the ^1H and ^{17}O nuclei are the same, *i.e.* the proton exchange rates are controlled by the exchange of water molecules in the aqueous solutions, of Co^{2+} and Fe^{2+}.

Paramagnetic relaxation of the CH_2 *protons.* The paramagnetic relaxation mechanism of the CH_2 protons studied may be different from that of water protons. Therefore temperature-dependent measurements were carried out on the cobalt(II)–glycinate, –ethylenediamine, and –malonate systems to reveal the mechanism of the relaxation. The temperature dependence of the paramagnetic relaxation rates and shifts in solutions of $[Co(glyO)_3]^-$, $[Co(en)_3]^{2+}$, and $[Co(mal)_2]^{2-}$ was detected (see Figure 2) in a concentration range where only one paramagnetic complex is dominant. The calculated activation and n.m.r. parameters for the $[Co(en)_3]^{2+}$, $[Co(mal)_2]^{2-}$, and $[Co(glyO)_3]^-$ are as follows: $\Delta H^\ddagger = 47 \pm 4$, 41 ± 4, and 43 ± 3 kJ mol^{-1}; $\Delta S^\ddagger = -21 \pm 11$, ≈ 0, and -37 ± 10 J K^{-1} mol^{-1}; $10^3\,\alpha = 7.2 \pm 0.2$, 10.7 ± 0.2, and 6.4 ± 1.5 K, respectively. The evaluation of the data by the temperature-dependent Swift–Connick equations[4] demonstrated that the relation $T_{2M}^{-1} \ll \Delta\omega_M$ applies to the CH_2 protons, too.

Table 2. Kinetic and n.m.r. parameters of $[Co(H_2O)_6]^{2+}$ and $[Fe(H_2O)_6]^{2+}$ (25 °C, I = 1 mol dm^{-3} KCl)

Parameter	$[Co(H_2O)_6]^{2+}$	Ref.^{a}	$[Fe(H_2O)_6]^{2+}$	Ref.
$10^{-6}k^{M-H_2O}/s^{-1}$	2.7 ± 0.1		3.1^b	2
	2.2^c	10	3.2^d	4
	2.4^e	18		
	1.1^d	4		
$\Delta H^\ddagger$/kJ mol^{-1}	45 ± 3		28.2^b	2
	43.1^c	10	$32.2^{a,d}$	4
	43.5^e	18		
	33.5^d	4		
$\Delta S^\ddagger$/J K^{-1} mol^{-1}	29 ± 7		-28^b	2
	21^c	10	$-12.3^{a,d}$	4
	22^e	18		
	-17^d	4		
$10^2\alpha$/K	2.32 ± 0.02		3.83	2
$10^{-3}r_{os}/s^{-1}$	1.8 ± 0.4		2.87^b	2

[a] Data measured using ^{17}O n.m.r. spectroscopy. [b] By proton spectroscopy. [c] In 2 mol dm^{-3} NH_4NO_3. [d] In 0.1 mol dm^{-3} $HClO_4$. [e] In $\approx$0.4 mol dm^{-3} $HClO_4$.

The relaxation processes of the complexes $[Co(glyO)_3]^-$ and $[Co(en)_3]^{2+}$ (at room temperature) are controlled by the chemical exchange, that of $[Co(mal)_2]^{2-}$ by the paramagnetic relaxation.

Kinetic Studies of the Cobalt(II) *Complexes.*—All the further measurements were carried out at constant temperature (25 °C), regulating the free-ligand concentration over a wide range of complex formation.

The measured paramagnetic relaxation data normalized for the total cobalt concentrations and the calculated curves are shown in the Figures together with the concentration distribution of the complexes. The calculated n.m.r. and kinetic parameters are collected in Table 3.

Ethylenediamine system. The detected relaxation rates (see Figure 3) over the whole range of complex formation can be interpreted in terms of the dissociation of the bis and tris complexes [equations (5) and (6)]. The mono complex did not

$$[Co(en)_2]^{2+} \overset{k_2^{d}}{\rightleftharpoons} [Co(en)]^{2+} + en \qquad (5)$$

$$[Co(en)_3]^{2+} \overset{k_3^{d}}{\rightleftharpoons} [Co(en)_2]^{2+} + en \qquad (6)$$

cause a measurable paramagnetic effect because the dissociation rate does not lie on n.m.r. time-scale. However, it is to be noted that $v = k_H^f[Co^{2+}][Hen^+]$, but no thermodynamic evidence can be given for the formation of the complex of the protonated ligand.

No paramagnetic shift could be detected over the whole complex-formation range; the relaxation processes are controlled by the chemical exchange [see equation (4); *i.e.* $\tau_M^{-2}/\Delta\omega_M$ is rather small if $\tau_M^{-1} \ll \Delta\omega_M$].

Malonate system. The rapid dissociation processes of the cobalt(II)–malonate complexes had a considerable contribution to the linewidth and shift. The measured data (see Figure 4) can be interpreted as a dissociation effect of the parent complexes [equations (7) and (8)] for which equilibrium data are available.

$$[Co(mal)] \overset{k_1^{d}}{\rightleftharpoons} Co^{2+} + mal^{2-} \qquad (7)$$

$$[Co(mal)_2]^{2-} \overset{k_2^{d}}{\rightleftharpoons} [Co(mal)] + mal^{2-} \qquad (8)$$

On increasing the free malonate concentration after the formation of the bis complex the relaxation effect of the supposed tris complex was detected [equation (9)]. The kinetics

Table 3. Kinetic and n.m.r. parameters of the cobalt complexes (25 °C, I = 1 mol dm^{-3} KCl)

Kinetic process	$10^{-3}\,r_{T2}^{-1}/s^{-1}$	$10^{-4}\,r_\omega$/rad s^{-1}	$10^{-3}\,k_d/s^{-1}$	$10^{-4}\,\Delta\omega_M$/rad s^{-1}
$Co^{2+} + Hen^+$	9 + 3*		9*	
$[Co(en)_2]^{2+} \rightleftharpoons [Co(en)]^{2+} + en$	0.59 ± 0.02		0.59	
$[Co(en)_3]^{2+} \rightleftharpoons [Co(en)_2]^{2+} + en$	3.06 ± 0.02		3.06	
$Co^{2+} + Hmal^-$		2.16 ± 0.21		
$[Co(mal)] \rightleftharpoons Co^{2+} + mal^{2-}$	7.64 ± 0.76	3.04 ± 0.46	129	3.18
$[Co(mal)_2]^{2-} \rightleftharpoons [Co(mal)] + mal^{2-}$	3.97 ± 0.38	3.14 ± 0.08	233	3.16
$[Co(mal)_2]^{2-} + mal^{2-}$	13.6 ± 1.4*	2.08 ± 0.23*		2.90*
$[Co(gly)]^+ \rightleftharpoons Co^{2+} + gly$	3.40 ± 0.06	1.70 ± 0.05	88.4	1.77
$[Co(glyO)_2] \rightleftharpoons [Co(glyO)]^+ + glyO^-$	0.39 ± 0.09		0.39	
$[Co(glyO)_3] \rightleftharpoons [Co(glyO)_2] + glyO^-$	1.30 ± 0.08		1.30	
$[Co(glyO)_3]^- + glyO^-$	4.22 ± 0.19*		4.22*	

* Second-order rate constants and n.m.r. parameters, because the equilibrium data are not known; only the kinetic data indicate the complex formation.

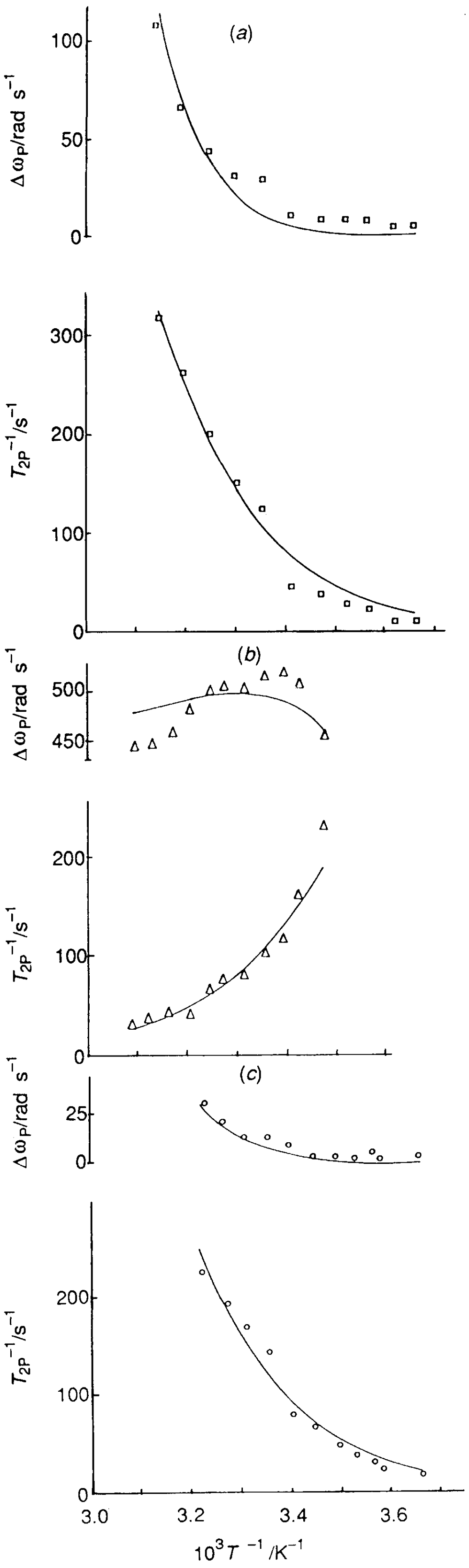

Figure 2. Temperature dependence of the paramagnetic relaxation rate and shift, together with the calculated curves, in solutions of (*a*) $[Co(en)_3]^{2+}$ ($P_{Co(en)_3} = 3.412 \times 10^{-2}$), (*b*) relaxation rate and shift in the solutions of $[Co(mal)_2]^{2-}$ ($P_{Co(mal)_2} = 1.133 \times 10^{-2}$), and (*c*) $[Co(glyO)_3]^-$ ($P_{Co(glyO)_3} = 6.875 \times 10^{-2}$)

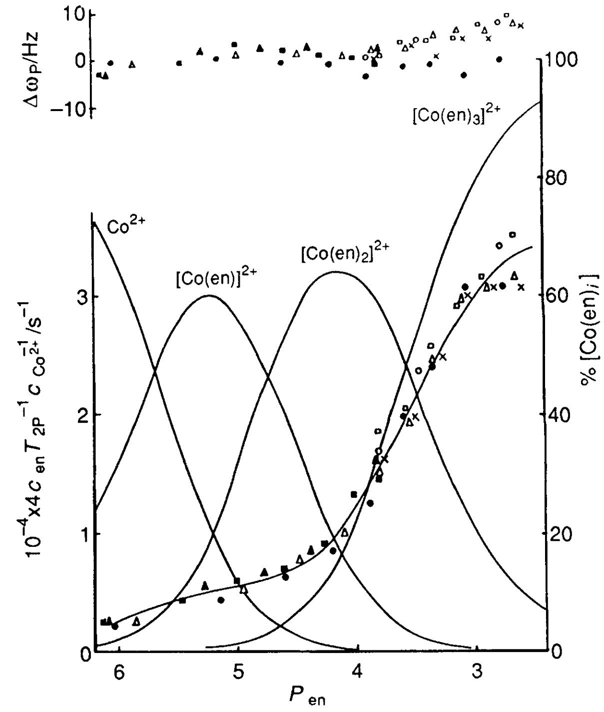

Figure 3. Normalized paramagnetic relaxation rate data for the cobalt(II)–ethylenediamine system detected for the CH_2 protons of the ligand, and the calculated curve together with the concentration distribution: $c_H{}^0 = 1.0466$, $c_{en}{}^0 = 0.5137$, $c_{Co}{}^0 = 0.005\,47$ (×), 0.007 30 (△), 0.009 12 (□), 0.013 68 (○), 0.018 25 (▲), 0.027 37 (■); $c_H{}^0 = 1.1266$, $c_{en}{}^0 = 0.5089$, $c_{Co}{}^0 = 0.018\,25$ mol dm^{-3} (●)

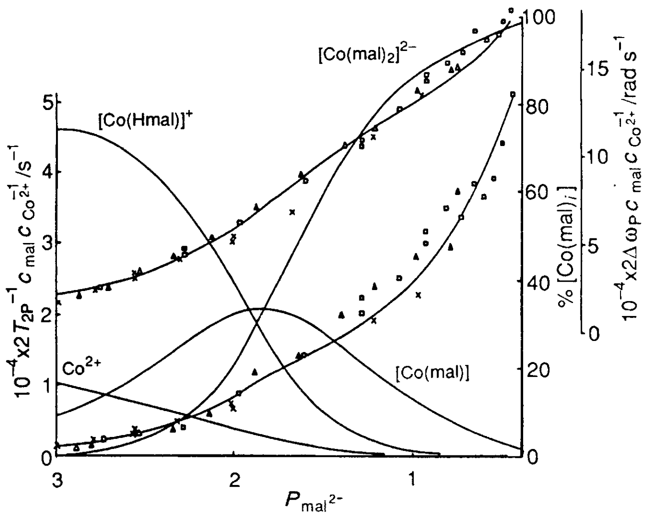

Figure 4. Normalized paramagnetic relaxation rate and shift data for the cobalt(II)–malonate system measured for the CH_2 protons of the ligand, and the calculated curves together with the concentration distribution: $c_H{}^0 = 0.7231$, $c_{mal}{}^0 = 0.5000$, $c_{Co}{}^0 = 0.001\,83$ (□), 0.007 30 (×); $c_H{}^0 = 0.5511$, $c_{mal}{}^0 = 0.4000$, $c_{Co}{}^0 = 0.003\,65$ (△), 0.018 25 mol dm^{-3} (○)

$$[Co(mal)_2]^{2-} + mal^{2-} \overset{k_3{}^f}{\rightleftharpoons} [Co(mal)_3]^{4-} \qquad (9)$$

parameter is given as a formation of the concentration of the product because no stability constant could be determined for $[Co(mal)_3]^{4-}$

The relaxation effect of the $[Co(Hmal)]^+$ complex could be calculated only from the chemical shift. However, no effect of

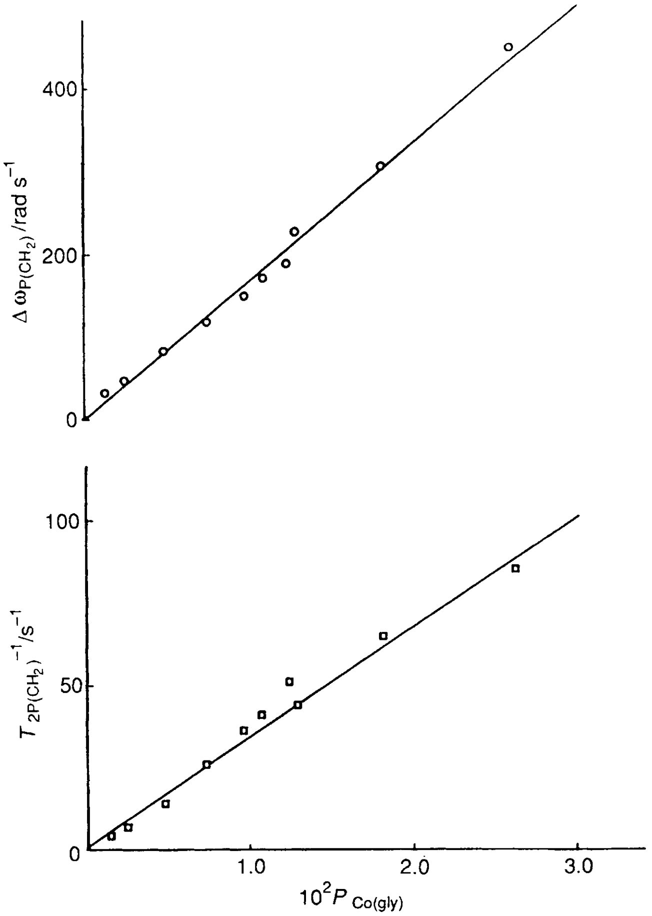

Figure 5. Paramagnetic relaxation effect of $[\mathrm{Co(gly)}]^{2+}$ detected for the $\mathrm{CH_2}$ protons of the ligand (pH 3.25)

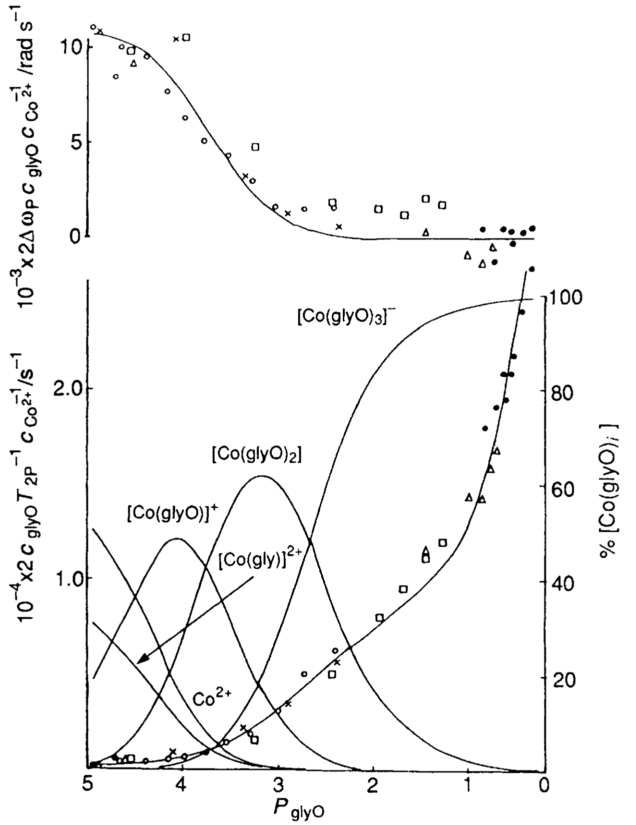

Figure 6. Normalized paramagnetic relaxation rate and shift data for the cobalt(II)–glycinate system measured on the $\mathrm{CH_2}$ protons of the ligand, and the calculated curves together with the concentration distribution: $c_{\mathrm{H}}^{0} = 1.5000$, $c_{\mathrm{glyO}}^{0} = 1.5000$, $c_{\mathrm{Co}}^{0} = 0.010\,54$ (□), 0.010 54 (△), 0.020 07 (●), 0.042 14 (×), 0.051 44 mol dm^{-3} (○)

this process was detected on the measured relaxation rates because of the strong relaxation control [see equation (3); *i.e.* $\Delta\omega_{\mathrm{M}}{}^{2}/\tau_{\mathrm{M}}{}^{-1}$ is rather small if $\tau_{\mathrm{M}}{}^{-1} \gg \Delta\omega_{\mathrm{M}}$], thus there are insufficient data for the calculation of the kinetics parameter.

Glycinate system. The dissociation rate of $[\mathrm{Co(glyO)}]^{+}$ is rather slow[6] and out of the range of the n.m.r. time-scale. The paramagnetic relaxation effect of the process (10) is shown in

$$[\mathrm{Co(gly)}]^{2+} \overset{k_{\mathrm{H}'}{}^{\mathrm{d}}}{\rightleftharpoons} \mathrm{Co}^{2+} + \mathrm{gly} \qquad (10)$$

Figure 5, which was determined at constant pH 3.25 where the protonated complex is dominant. The relaxation contributions were calculated from the slopes. The kinetic and relaxation parameters were separated using equations (3) and (4).

For the description of the experimental data in the complex formation range (see Figure 6) the dissociation processes (11)

$$[\mathrm{Co(glyO)_2}] \overset{k_2{}^{\mathrm{d}}}{\rightleftharpoons} [\mathrm{Co(glyO)}]^{+} + \mathrm{glyO}^{-} \qquad (11)$$

and (12) were considered. Increasing the free glycinate

$$[\mathrm{Co(glyO)_3}]^{-} \overset{k_3{}^{\mathrm{d}}}{\rightleftharpoons} [\mathrm{Co(glyO)_2}] + \mathrm{glyO}^{-} \qquad (12)$$

concentration after the formation of the tris complex resulted in a sharp change on the relaxation rate: $v = k_4{}^{\mathrm{f}}[\mathrm{Co(glyO)_3}^{-}][\mathrm{glyO}^{-}]$. The relaxation of $[\mathrm{Co(glyO)_2}]$ and $[\mathrm{Co(glyO)_3}]^{-}$ is controlled by the chemical exchange ($\tau_{\mathrm{M}}{}^{-1} \ll \Delta\omega_{\mathrm{M}}$); the paramagnetic shift could not be detected because the $\tau_{\mathrm{M}}{}^{-2}/\Delta\omega_{\mathrm{M}}$ value [see equation (4)] is rather small. The change of the paramagnetic shift over the whole range can be attributed to the formation of $[\mathrm{Co(gly)}]^{2+}$.

The formation rate constants of the complexes of Co^{2+} and Fe^{2+} measured in our laboratory together with the earlier literature data are collected in Table 4. The rate constants of the bis- and tris-glycinato cobalt complexes agree well with the literature data determined by the chemical relaxation (*T*-jump) method. The considerable difference between the literature and our formation rate constants for the monomalonato complex can be partly explained by the high sensitivity to the small stability constant under the different experimental conditions. Comparison of our formation rate constant for $[\mathrm{Co(en)_3}]^{2+}$ with the literature data is rather clumsy because no correct analysis of the stability constants and the relaxation properties is available in the earlier papers.[11,12]

The stability constants of the outer-sphere complexes (K_{os}) could be calculated in the case of cobalt(II)–glycinate and –malonate complexes using literature water-exchange rate constants (see Table 4). For the formation of $[\mathrm{M(en)}]^{2+}$ only estimated lower K_{os} limits could be given {the $k_1{}^{\mathrm{f}}$ value is unknown in the case of $[\mathrm{Co(en)}]^{2+}$} supposing that the formation rate constant is not smaller than that for the bis complex and $k^{\mathrm{M(H_2O)_6}}$ water-exchange rate constants were used for the calculation. No water-exchange rate constants are available for the cobalt(II)–ethylenediamine complexes, therefore no K_{os} values can be calculated for the bis and tris complexes. Strong outer-sphere association was observed in the formation of $[\mathrm{Co(mal)}]$, $[\mathrm{Fe(mal)}]$, $[\mathrm{Co(en)}]^{2+}$, and [Fe-

Table 4. Formation rate constants and K_{os} values for the complexes of Co^{2+} and Fe^{2+} ($K_{os} = k^f/k^{M-H_2O\,a}$) at 25 °C and I = 1 mol dm^{-3} KCl

Complex or kinetic process	$k^f[CoL_i]$/ dm^3 mol^{-1} s^{-1}	Ref.	$k^f[FeL_i]$/ dm^3 mol^{-1} s^{-1}	Ref.	K_{os}/dm^3 mol^{-1}	
					$[CoL_i]$	$[FeL_i]$
M^{2+} + Hen^+	$(9 \pm 3) \times 10^3$		1.5×10^4	2		
$[M(en)(H_2O)_4]^{2+}$			7.1×10^7	2	$>11^b$	22.2^b
$[M(en)_2(H_2O)_2]^{2+}$	$(3.03 \pm 0.09) \times 10^7$		1.8×10^7	2		
$[M(en)_3]^{2+}$	$(1.11 \pm 0.01) \times 10^7$		2.1×10^6	2		
	2.0×10^{6c}	12				
	6.3×10^{6c}	11				
M^{2+} + $Hmal^-$			4.2×10^5	2		
$[M(mal)(H_2O)_4]$	$(6.9 \pm 1.0) \times 10^7$		6.8×10^7	2	25.7	21.3
	9×10^6	9			3.33	
$[M(mal)_2(H_2O)_2]^{2-}$	$(1.6 \pm 0.2) \times 10^7$		1.3×10^7	2	0.73	
$[M(mal)_2]^{2-}$ + mal^{2-}	$(4.7 \pm 0.5) \times 10^4$				$<5 \times 10^{-4}$	
$[M(gly)]^{2+}$	$(8.8 \pm 0.2) \times 10^4$					
$[M(glyO)(H_2O)_4]^+$	1.5×10^{6c}	6	5.4×10^6	2	0.56	1.7
	3.0×10^{6c}	7			1.11	
$[M(glyO)_2(H_2O)_2]$	$(2.2 \pm 0.5) \times 10^6$		5.0×10^6	2	0.50	
	2.0×10^{6c}	6			0.74	
	2.2×10^{6c}	8			0.50	
$[M(glyO)_3]^-$	$(6.4 \pm 0.4) \times 10^5$		1.9×10^6	2	0.24	
	8.0×10^{5c}	6	$4.0 \times 10^{4c,d}$	2	0.30	
	9.0×10^{5c}	8			0.33	
	2.0×10^{6c}	11				
$[M(glyO)_3]^-$ + $glyO^-$	$(4.2 \pm 0.2) \times 10^4$		4.7×10^4	2		

[a] k^{Co-H_2O}/s^{-1}: $[Co(glyO)(H_2O)_4]^+$, 4.4×10^6;[8] $[Co(glyO)_2(H_2O)_2]$, 8.6×10^6;[8] $[Co(mal)(H_2O)_4]$, 2.2×10^7;[10] $[Co(mal)_2(H_2O)_2]^{2-}$, $>1 \times 10^8$.[10] [b] Estimated value. [c] I = 0.1,[6] 0.2 mol dm^{-3} $NaNO_3$;[7] 0.1 mol dm^{-3} KNO_3;[8] 1 mol dm^{-3} $NaNO_3$.[11] [d] Given for $[Fe(glyO)_2]$ + $glyO^-$ exchange reaction.

(en)]$^{2+}$, which can be attributed to the two negative charges of the mal^{2-} and to the internal conjugate base mechanism[19] of the en ligand co-ordination. The K_{os} (and k^f) values for [M(mal)] seem higher than expected, however we have no explanation for this.

According to the similar kinetic behaviour of $[Co(H_2O)_6]^{2+}$ and $[Fe(H_2O)_6]^{2+}$ the mechanism of formation of their complexes (with ligands without specific interactions) are probably similar. It is seen from Table 4 that the formation rate constants of the complexes of Co^{2+} and Fe^{2+} are similar. On changing the structure and the charge of the ligands the formation rate constants of their complexes alter in the same direction. Nevertheless, comparison of the dissociation rate constants (see data in Table 3 and ref. 2) shows the higher lability of the iron complexes.

Despite the revealed thermodynamic and kinetic differences (a greater degree of covalent bonding in the cobalt complexes[5] and the higher lability of the iron complexes[2]) the mechanism of formation mechanism of complexes of these two metal ions seems to be similar.

Only kinetic evidence could be given for the formation of $[Co(Hen)]^{3+}$, $[Co(Hmal)]^+$, and $[Co(mal)_3]^{4-}$. The rather slow formation rate constants of $[Co(mal)_3]^{4-}$ is in accord with the charge product of the species involved.

The interaction between $(Co(glyO)_3]^-$ and free $glyO^-$ is not a precedent for this type of reaction. Similar kinetic processes were detected between $[Fe(glyO)_3]^-$ and free $glyO^-$ as well as $[Cr(ida)_2]^{2-}$ and ida^{2-} (ida = iminodiacetate) in our earlier works.[2,3] All these processes could be explained by the 'carboxyl displacement'.[2] The nitrogen-donor group of the free ligand can displace the more weakly bonded carboxyl group from the chelate ring, forming formally a complex with two chelate and two monodentate ligands. The crammed co-ordination sphere of these complexes is distorted which results in a low stability and high lability. pH-Metry and spectrophotometry are not suitable for the determination of these small formation constants. Taking into account the experimental results the 'carboxyl-displacement' mechanism seems to provide a correct interpretation.

Acknowledgements

We thank Mrs. Istránné Bíró for experimental work.

References

1 I. Nagypál, K. Micskei, and F. Debreczeni, *Inorg. Chim. Acta*, 1983, **77**, L161.
2 K. Micskei and I. Nagypál, *J. Chem. Soc., Dalton Trans.*, 1990, 743.
3 K. Micskei and I. Nagypál, *J. Chem. Soc., Dalton Trans.*, 1990, 1301.
4 T. J. Swift and R. E. Connick, *J. Chem. Phys.*, 1962, **37**, 307.
5 K. Micskei, *J. Chem. Soc., Dalton Trans.*, 1987, 255.
6 G. Davies, K. Kustin, and R. F. Pasternack, *Inorg. Chem.*, 1969, **8**, 1535.
7 M. W. Grant, *J. Chem. Soc., Faraday Trans. 1*, 1973, 69.
8 G. G. Hammes and J. I. Steinfeld, *J. Am. Chem. Soc.*, 1962, **84**, 4639.
9 F. P. Cavasino, *Ric. Sci.*, 1965, **8**, 1120.
10 P. E. Hoggard, H. W. Dodgen, and J. P. Hunt, *Inorg. Chem.*, 1971, **10**, 959.
11 R. G. Pearson and R. D. Lanier, *J. Am. Chem. Soc.*, 1964, **86**, 765.
12 F. Basolo, *Adv. Chem. Ser.*, 1965, **49**, 81.
13 A. E. Martell and R. E. Smith, 'Critical Stability Constants,' Plenum, New York and London, 1975—1982, vols. 1—5.
14 H. Irving, M. G. Miles, and L. D. Pettit, *Anal. Chim. Acta*, 1967, **38**, 475.
15 L. Zékány and I. Nagypál, 'Computational Methods for the Determination of Formation Constants,' ed. D. J. Leggett, Plenum, New York, 1985, p. 291.
16 I. Fábián and I. Nagypál, *Talanta*, 1982, **29**, 71.
17 Y. Kuroda and H. Aiba, *J. Am. Chem. Soc.*, 1979, **101**, 6837.
18 A. M. Chmelnick and D. Fiat, *J. Chem. Phys.*, 1967, **47**, 3986.
19 D. B. Rorabacher, *Inorg. Chem.*, 1966, **5**, 1891.

Received 3rd *October* 1989; *Paper* 9/04223G